NeuroImage 254 (2022) 119118

Contents lists available at ScienceDirect

NeuroImage

journal homepage: www.elsevier.com/locate/neuroimage

Comparing brain asymmetries independently of brain size

Camille Michèle Williams[a,*,†], Hugo Peyre[a,b,c], Roberto Toro[d], Franck Ramus[a]

[a] Laboratoire de Sciences Cognitives et Psycholinguistique, Département d'Études Cognitives, École Normale Supérieure, EHESS, CNRS, PSL University, 75005 Paris, France
[b] INSERM UMR 1141, Paris Diderot University, Paris, France
[c] Department of Child and Adolescent Psychiatry, Robert Debré Hospital, APHP, Paris, France
[d] Institut Pasteur, Université de Paris, Unité de neuroanatomie appliquée et théorique, Paris, France

ARTICLE INFO

Keywords:
Brain asymmetry
Brain volume
Cortical thickness
Cortical surface area
Sex
Age

ABSTRACT

Studies examining cerebral asymmetries typically divide the L-R Measure (e.g., Left–Right Volume) by the $L + R$ Measure to obtain an Asymmetry Index (AI). However, contrary to widespread belief, such a division fails to render the AI independent from the $L + R$ Measure and/or from total brain size. As a result, variations in brain size may bias correlation estimates with the AI or group differences in AI. We investigated how to analyze brain asymmetries in to distinguish global from regional effects, and report unbiased group differences in cerebral asymmetries in the UK Biobank ($N = 40,028$).

We used 306 global and regional brain measures provided by the UK Biobank. Global gray and white matter volumes were taken from Freesurfer ASEG, subcortical gray matter volumes from Freesurfer ASEG and subsegmentation, cortical gray matter volumes, mean thicknesses, and surface areas from the Destrieux atlas applied on T1-and T2-weighted images, cerebellar gray matter volumes from FAST FSL, and regional white matter volumes from Freesurfer ASEG.

We analyzed the extent to which the $L + R$ Measure, Total Cerebral Measure (TCM, e.g., Total Brain Volume), and L-R TCM predict regional asymmetries. As a case study, we assessed the consequences of omitting each of these predictors on the magnitude and significance of sex differences in asymmetries.

We found that the $L + R$ Measure, the TCM, and the L-R TCM predicted the AI of more than 89% of regions and that their relationships were generally linear. Removing any of these predictors changed the significance of sex differences in 33% of regions and the magnitude of sex differences across 13–42% of regions. Although we generally report similar sex and age effects on cerebral asymmetries to those of previous large-scale studies, properly adjusting for regional and global brain size revealed additional sex and age effects on brain asymmetry.

Abbreviations

L	Left Hemisphere
R	Right Hemisphere
AI	Asymmetry Index = (L-R)/($L + R$)
TBV	Total Brain Volume
TSA	Total Surface Area
Total MCT	Total Mean Cortical Thickness
TCM	Total Cerebral Measure (i.e., TBV or TSA or Total MCT)
Measure	Volume, Mean Thickness, Surface Area
$L + R$	$L + R$ Measure
L-R	L-R Measure
L-R TCM	L-R Total Cerebral Measure (i.e., L-R TBV or TSA or Total MCT)

1. Introduction

Symmetry is a central feature of human brain structure. But symmetry is not perfect. Despite global symmetry, numerous neuroanatomical asymmetries have been documented (de Kovel et al., 2017; Ocklenburg et al., 2017; Toga and Thompson, 2003) and appear to have functional significance (Altarelli et al., 2014; Cherbuin et al., 2010; Mazoyer et al., 2014; Zago et al., 2017). These cerebral asymmetries occur across subcortical (e.g., Guadalupe et al., 2017), cortical (e.g., Kavaklioglu et al., 2017; X.-Z. Kong et al., 2018, 2020), and cerebellar (e.g., (Kavaklioglu et al., 2017; F. Kurth et al., 2018) volumes, as well as cortical surface areas and thicknesses (e.g., X.-Z. Kong et al., 2018; Luders et al., 2006; Maingault et al., 2016; Plessen et al., 2014). Although some anatomical features are lateralized at the population level, asymmetry is a complex multivariate trait affected by a number

* Corresponding author at: École Normale Supérieure, 29 rue d'Ulm.
† ORCID.
E-mail address: camille.williams@ens.psl.eu (C.M. Williams).
URL: https://orcid.org/0000-0002-1471-6566 (C.M. Williams)

https://doi.org/10.1016/j.neuroimage.2022.119118.
Received 10 December 2021; Received in revised form 17 March 2022; Accepted 18 March 2022
Available online 19 March 2022.

of factors including age, sex, and psychiatric disorders (for review see Kong et al., 2020). Accurately quantifying these variations across populations, may shed a light on the complex relationship between brain asymmetries and behavior.

Brain asymmetries are typically calculated by dividing the difference between the left and right measures (e.g., volume) of a region by their sum: AI = (Left-Right Measure) / (Left+Right Measure), with the measure corresponding to volume, mean thickness, or surface area (e.g., Galaburda et al., 1987; Kong et al., 2020; F. Kurth et al., 2018). Although studies on brain asymmetry generally do not explain why they divide L-R by $L + R$ (e.g., Guadalupe et al., 2017; X.-Z. Kong et al., 2018; Leonard et al., 1993; Zuo et al., 2019), some suggest that the denominator at least partially controls for head size (e.g., Galaburda et al., 1987; Steinmetz et al., 1989) or that it "ensures that the index does not simply scale with brain size" (Kong et al., 2020). This adjustment is similar to the proportion method, a method used to adjust for differences in brain size that divides a regional measure (e.g., hippocampal volume) by a Total Cerebral Measure (TCM; e.g., Total Brain Volume (TBV)). However, instead of removing the effect of brain size on the local measure, studies have shown that the proportion approach often inverts the effect of brain size because it assumes that the intercept of the relationship between a local measure and brain size is null and that the relationship is linear[1] (Lefebvre et al., 2015; Liu et al., 2014; Sanchez-Roige et al., 2019). Since the intercept is generally not null, dividing by the global measure can lead to reporting inaccurate group differences (Reardon et al., 2016; Sanchis-Segura et al., 2019; Williams et al., 2021a, 2021b). To take this issue into account, recent studies adjust for brain size by using the covariate approach, which includes the global measure as a covariate in the linear regression models. This raises the question of whether bilateral ($L + R$) measures and/or global brain size should also be considered as covariates when examining group differences in asymmetry.

Furthermore, the covariate approach, like the proportion method, assumes that the relationship between a local and a global measure is linear, while a growing literature suggests that the relationships between global and local cerebral measures are non-linear (Finlay et al., 2001; Fish et al., 2017; Reardon et al., 2016; P.K. 2018; Toro et al., 2009). Thus, ignoring non-linearities in the brain could additionally lead to reporting inaccurate group differences.

Finally, global brain asymmetry may also influence local brain asymmetries. Although global brain asymmetries have been investigated across studies linking neuroanatomy to cognition and mental health disorders, the relationship between the global and local AI remains unclear. As global brain asymmetries may partly explain local asymmetries, omitting the L-R TCM could influence reported group differences in asymmetries.

In the present paper, we aimed to identify the brain measures that should be taken into account by studies examining group differences in cerebral asymmetries. We first examined whether the $L + R$ Measure, TCM, and L-R TCM significantly predicted regional asymmetries. We then investigated whether the relationship between the regional AI and the $L + R$ Measure, global brain size, and the L-R TCM were non-linear. Thirdly, since the two sexes differ in brain size, we used the case of sex differences in brain asymmetries to illustrate the consequences of not taking these adjustments into account. Finally, we reported the effects of sex, age, and their interactions when including all necessary brain covariates to report group differences in asymmetries that do not scale with brain size.

[1] Consider Left (L) and Right (R) measures for a given region. L is regressed on R, with a>0: L=aR+b (error term removed for simplicity). If L and R are correlated and a<1 then L-R= (a-1)R + b will be negatively correlated with R and dividing by L + R will not remove this correlation: AI=(L-R)/(L + R)= ((a-1)R + b)/((a + 1)R + b). Therefore, the nature of the relationship with R depends on the values of a and b. Since the AI is correlated with R in most cases, it will also be correlated with L + R.

2. Methods

2.1. Participants

We included UK Biobank participants that completed a Magnetic Resonance Imaging (MRI) (N ≃ 41,000). In brief, the UK Biobank is an open-access large prospective study with phenotypic, genotypic, and neuroimaging data that includes 500 000 participants recruited between 2006 and 2011 at 40 to 69 years old in Great Britain (Sudlow et al., 2015). All participants provided informed consent ("Resources tab" at https://biobank.ctsu.ox.ac.uk/crystal/field.cgi?id=200). The UK Biobank received ethical approval from the Research Ethics Committee (reference 11/NW/0382) and the present study was conducted under application 46 007.

The neuroimaging phenotypes in this study correspond to volumes, mean thicknesses, surface areas from the first imaging visit (Instance 2) and were generated by an image-processing pipeline developed and run by the UK Biobank Imaging team (Alfaro-Almagro et al., 2018; Miller et al., 2016).

2.1.1. Brain image acquisition and processing

A standard Siemens Skyra 3T running VD13A SP4 with a standard Siemens 32-channel RF receive head coil was used to collect data (Brain Scan Protocol). The 3D MPRAGE T1-weighted volumes were analyzed by the UK Biobank Imaging team with pipeline scripts that primarily call for FSL and Freesurfer tools. Details of the acquisition protocols, image processing pipeline, image data files, and derived measures of brain structure and function are available in the UK Biobank Imaging Protocols.

2.1.2. Total brain volume (TBV)

TBV was calculated as the sum of the following ASEG segmentation: Cerebellum GMV (Left: 26,557, Right: 26,588), Cerebral GMV (Left: 26,552, Right: 26,583), Cerebellum WMV (Left: 26,556, Right: 26,587), Cerebral WMV (Left: 26,553, Right: 26,584), and the total subcortical volume we calculated with the ASEG and Freesurfer subfields. Refer to Supplemental Section 1 for details on the choice of TBV. We excluded individuals with missing data in these regions, yielding 40 055 participants.

2.1.3. Scanner site

The age and sex of participants differed across the 3 scanner sites located in Cheadle (Site 11,025), Reading (Site 11,026), and Newcastle (Site 11,027; Supplemental Section 2). One individual without scanner site location was removed from the analyses, yielding 40 054 participants.

2.1.4. Sex

Participants who did not self-report as male or female or whose self-reported sex and genetic sex differed were also excluded from the analyses ($N = 26$). When genetic sex was not available, reported sex was used to define the sex of the participant. Of the 40 028 participants included in the analyses, there were more females ($N = 21\,142$) than males ($N = 18\,886$, $\chi^2(1) = 127.15$, $p < 2.2e\text{-}16$).

2.1.5. Age

To obtain a continuous measure of age, age was calculated based on the year and month of birth of the participant and the day, month, and year of their MRI visit. The mean age was 64.13 years old ($SD = 7.54$). Males ($M = 64.81$ years, $SD = 7.64$) were older than females ($M = 63.51$ years, $SD = 7.39$, $t_{(39,186)} = 17.17$, $p < 2.2e\text{-}16$).

2.1.6. Handedness

Handedness was measured with a multiple-choice self-report question "Are you right or left-handed?" (data field 1707). The age and sex of participants differed between Right-handed ($N = 35,596$), Left-handed

($N = 3711$), and ambidextrous ($N = 547$) individuals (Supplemental Section 3). Participants without handedness data ($N = 174$) were excluded from the analyses in Q4.

2.2. Brain measures

The descriptive statistics of all global and regional brain measures analyzed in the present study and their respective data fields and segmentation origin are listed in Supplemental Tables A1–5. Brain measures mainly correspond to GMV since WMVs were not segmented by the UK Biobank Imaging Team.

2.2.1. Global brain measures

A total of 10 Global AIs were investigated: Hemispheric Brain Volume, Mean Cortical Thickness, Surface Area, Subcortical GMV, Cortical GMV, Cerebral GMV, Cerebral WMV, 2 measures of Cerebellar GMV (ASEG and FAST FSL), and Cerebellar WMV. We examined two measures of Cerebellar GMV to evaluate the consistency of the FAST FSL and ASEG segmentation algorithms since we previously found sex effects in the opposite direction between the ASEG and the FAST FSL Cerebellar GMVs (Williams et al., 2021a).

WMV measures were taken from the left and right Freesurfer ASEG segmentation (category 190). The left and right Cerebellum GMV measures correspond to the sum of the left and right cerebellar volumes from the FAST segmentation (category 1101) and the left and right ASEG Cerebellum GMVs (Left: data-field 26,557, Right: data-field 26,588).

Following the recommendations from the UK Biobank Imaging Protocols, we excluded Freesurfer brain measures when T2-FLAIR was not used with the T1 images for the Freesurfer a2009s (volume, surface area, and mean thickness) and Freesurfer subfield segmentations. The left and right Total Mean Cortical Thicknesses (MCT) and Total Surface Area (TSA) respectively corresponded to the left and right mean cortical thickness and surface area measures from the Freesurfer a2009s segmentation (category 197). Participants that were missing more than 10% of the mean cortical thicknesses were excluded from the mean thickness analyses. The same criterion was applied to surface areas. The left and right Cortical GMVs correspond to the sum of the left and right volumetric measures from the Freesurfer a2009s segmentation (category 197) and the Cerebral GMV corresponds to the ASEG Cerebral GMVs (Left: data-field 26,552, Right: data-field 26,583). The Subcortical GMV was calculated from the sum of the left and right whole amygdala, hippocampus, and thalamus volumes from the Freesurfer subfields (category 191) and the left and right caudate, accumbens, pallidum, ventral diencephalon, and putamen of the Freesurfer ASEG segmentation (category 190).

While 40 028 individuals were included in the analyses, 39 238 individuals were included in the FAST segmentation analyses and 38 710 in the Freesurfer a2009s segmentation and subcortical subfields analyses. Missing values and null segmentations (e.g., 0 mm3) for a region were replaced by the mean of that region when calculating global measures.

2.2.2. Regional brain measures

A case-wise participant exclusion strategy was applied to each brain measure for the regional analyses: participants with a missing value or a segmentation error for a region were excluded from the analyses of that region but were maintained in the analyses of other brain measures. Following visual examination of the distribution of regional cerebral measures, values 3 times the interquartile range for a region were considered to be segmentation errors and were removed from the analyses of that region as done by Williams and colleagues (2021).

A total of 296 regional AIs were investigated: 222 cortical regions (74 vol, 74 surface areas, and 74 cortical mean thicknesses) from the Freesurfer a2009s segmentation (Destrieux Atlas, category 197), 56 whole segmentation and subfields of the amygdala, hippocampus, and thalamus (Freesurfer subfields, category 191), 10 cerebellum gray matter segmentation from the FAST segmentation (category 1101), and 8 subcortical and ventricle volumes from the Freesurfer ASEG segmentation (category 190). When choices between different types of segmentation were available, we took the smallest segmentation available (e.g. FreeSurfer Tools subfields) to obtain a finer grain analysis.

2.3. Statistical analyses

Analyses were preregistered on OSF and run using R (R Core Team, 2019). The preregistration and code are on OSF (https://osf.io/wt6uf). Packages are listed in Supplemental Section 7. The categorical sex variable was coded −0.5 for males and 0.5 for females. The scanner site was dummy coded with the largest site (Cheadle: Site 1102) as reference and handedness was dummy coded with the right-handed individuals as the reference.

2.3.1. Q1: do the L + R measure, global brain size, and the L-R TCM predict $AI_{regional}$?

The regional and the global asymmetry index were calculated as AI = (L-R Measure) / ($L + R$ Measure)). We tested whether the $L + R$ Measure, the TCM (TCM), and the L-R TCM significantly predicted the AI by applying Eq. (1) to each region/global measure. For global measures, the TCM corresponded to Total Brain Volume. For regional measures, the TCM was TBV when examining AIs of volumes, TSA for surface areas, and Total MCT for mean thicknesses.

$$\begin{aligned} AI = {} & \text{Intercept} + b_1 * (\text{L} + \text{R Measure}) + b_2 * (\text{TCM}) + b_3 * (\text{L} - \text{R TCM}) \\ & + b_4 * \text{Scanner Site} + \text{error} \end{aligned} \quad (1)$$

We tested the effect of a given covariate on regional AIs at a threshold of 0.05 and then evaluated whether more regions than expected by chance (given the alpha) show a significant effect of this covariate. Therefore, if any predictor significantly predicted the AI (alpha = 0.05) in more than 5% of regional and global measures, we concluded that the predictor should be included when examining group differences in asymmetry. A significant $L + R$ Measure suggested that the regional AI did not properly adjust for the $L + R$ Measure.

Even if dividing by $L + R$ did not properly adjust for $L + R$, we kept defining the AI as (L-R Measure)/($L + R$ Measure) instead of defining it as the L-R Measure to obtain a comparable AI across regions.

2.3.2. Q2: is the relationship of the AI with the L + R measure, TCM, or the L-R TCM, non-linear?

Predictors included in the following models were based on the results from Q1. Here, we provide equations for the case where the $L + R$ Measure, TCM, and the L-R TCM significantly predict 95% or more AIs.

We compared a linear model (Eq. (1)) to standard nonlinear models (equations 2–7): polynomial linear regressions and splines. Equations are provided in supplemental section 4. The comparison was based on the percent change in Residual Standard Error (RSE) between the models[2]. The RSE is the square root of the residual sum of squares divided by the degrees of freedom and is provided in the output of each model using the summary function.

Since more complex models always yield lower RSE, we consider a "significantly better fit" as a reduction of RSE greater than 1%. If the reduction in RSE was larger than 1% in more than 5% of regional and global measures, this justified the use of the non-linear model over the linear one in the subsequent analyses.

The most common splines were selected based on Perperoglou and colleagues' (A. 2019) review and previous studies examining nonlinearities in neuroimaging studies (e.g., Fjell et al., 2009; P.K. Reardon et al., 2018). We used the gam function from the mgcv package (Wood, 2017) to model splines. The s() function will be applied to each predictor in the model for which we want a smoothing parameter.

From the results of Q1 and Q2, we determined a "default model for the analysis of brain asymmetries independent of brain size", including all the predictors determined by Q1, and the best linear or nonlinear

model determined by Q2. We then analyzed the consequences of departing from this default model with the case of sex differences in Q3.

2.3.3. Q3: to what extent do group estimates change with the included covariates?

We used sex as our grouping variable and generated Eqs. (8)-11 based on the results from Q1 and Q2. For instance, if Q1 showed that the $L + R$ Measure, the TCM, and the L-R TCM were significant predictors of the AIs and Q2 that the reduction in RSE across models was smaller than 1% for 95% or more of the AIs, we ran Eq. (8) as the default equation and compared it to equations removing one term at a time Eq. (9)-(11). We mean-centered and divided continuous variables by 1 SD to obtain standardized beta estimates (ß).

$$(\textbf{defaultmodel}) : \mathrm{AI} = \mathrm{Intercept} + \pi_1 * (\mathrm{Sex}) + \pi_2 * (\mathrm{TCM}) + \pi_3 (\mathrm{L-R\ TCM}) + \pi_4 * (\mathrm{L+R\ Measure}) + \pi_5 * (\mathrm{Scanner\ Site}) + \mathrm{error} \quad (8)$$

$$(\textbf{default model without L-RTCM adjustment}) : \mathrm{AI} = \mathrm{Intercept} + \pi_1 * (\mathrm{Sex}) + \pi_2 * (\mathrm{TCM}) + \pi_3 * (\mathrm{L+R\ Measure}) + \pi_4 * (\mathrm{Scanner\ Site}) + \mathrm{error} \quad (9)$$

$$(\textbf{default model without TCM adjustment}) : \mathrm{AI} = \mathrm{Intercept} + \pi_1 * (\mathrm{Sex}) + \pi_2 * (\mathrm{L-R\ TCM}) + \pi_3 * (\mathrm{L+R\ Measure}) + \pi_4 * (\mathrm{Scanner\ Site}) + \mathrm{error} \quad (10)$$

$$(\textbf{default model without L+R Measure adjustment}) : \mathrm{AI} = \mathrm{Intercept} + \pi_1 * (\mathrm{Sex}) + \pi_2 * (\mathrm{L-R\ TCM}) + \pi_3 * (\mathrm{TCM}) + \pi_4 * (\mathrm{Scanner\ Site}) + \mathrm{error} \quad (11)$$

We systematically compared the full model (Eq. (8)) with each subsequent model omitting one type of adjustment. For each pair of models considered, we statistically tested the difference in the sex coefficient ß1 at the alpha=0.05 level by conducting a Z-test, in all regions. For instance, for Eqs. (8) and 9, we computed the Z-score as follows:

$$Z = \left(\pi 1_{\mathrm{Equation8}} - \pi 1_{\mathrm{Equation9}}\right) / \mathrm{square\ root}\left(\left(\mathrm{SE}_{\mathrm{Equation8}}\right)^2 + \left(\mathrm{SE}_{\mathrm{Equation9}}\right)^2\right)$$

If the |Z-score| was greater or equal to 1.96, then the ß1 of the equations significantly differed at alpha = 0.05. If this test was significant in more than 5% of regional and global measures, we concluded that the omitted covariate led to incorrect estimations of sex differences in asymmetry.

2.3.4. Q4: do cerebral asymmetries vary as a function of age and sex effects and interactions?

We then examined sex differences in asymmetries by applying the model adjustments determined in Q1 and Q2 and by taking into account the effects of age on brain measures, as is commonly done in the literature.

In the case where (i) the $L + R$ Measure, the TCM, and the L-R TCM are significant predictors of AI and (ii) the percent change in RSE is smaller than 1% for 95% or more of the regional and global measures, we examined age (linear and quadratic) and sex effects and age by sex interactions with Eq. (12). We mean-centered and divided continuous variables by 1 SD to obtain standardized beta estimates. We used polynomials instead of splines to obtain a standardized beta coefficient for non-linear age effects and the non-linear age by sex interactions.

$$\begin{aligned}\mathrm{AI} = {} & \mathrm{Intercept} + \pi_1 * (\mathrm{L+R\ Measure}) \\ & + \pi_2 * (\mathrm{TCM}) \\ & + \pi_3 * (\mathrm{L-R\ TCM}) \\ & + \pi_4 * (\mathrm{Sex}) + \pi_5 * (\mathrm{age}) + \pi_6 * \left(\mathrm{age}^2\right) \\ & + \pi_7 * (\mathrm{sex}) \times (\mathrm{age}) + \pi_8 * (\mathrm{sex}) \times \left(\mathrm{age}^2\right) \\ & + \pi_9 * (\mathrm{handedness}) + \pi_{10} * (\mathrm{Scanner\ Site}) + \mathit{error}\end{aligned} \quad (12)$$

Multiple Comparison Corrections. Three thresholds of significance will be provided and will vary depending on the number of cerebral measures (296 regional measures and 10 global measures) and the number of estimates of interests in the performed regressions: $\alpha 1 = 0.05/$ (5 estimates of interest in regression), $\alpha 2 = 0.05/$ (306 cerebral measures), and $\alpha 3 = 0.05/$ (5 estimates of interest in regression * 306 cerebral measures).

Additional Analyses. We report the magnitude and significance of the AIs in Supplemental Tables A6. We created in Global Asymmetry Markers, Person-level Asymmetry Deviance Markers, Global Deviance Markers, and tested the Sex Difference in the Variance of the regional AIs in the Supplemental Section 6. Finally, we compared our raw AIs and sex and age effects to previous large-scale studies. We used cortical Desikan-Killiany segmentations to facilitate comparison with previous studies. More details on the method and the results are available in Supplemental Section 6.

3. Results

3.1. Q1: do the L + R measure, TCM size, and the L-R TCM predict the AI?

The $L + R$ Measure and the TCM significantly predicted 89% of global and regional AIs and the L-R TCM significantly predicted 96% of global and regional AIs (respectively, 271/306, 290/305, and 270/305). Estimates and p-values are reported in Supplemental Tables B1–4.

Across global measures, where TBV was the TCM, the $L + R$ TCM predicted the asymmetry in TBV, and the $L + R$ Measure, the L–R TCM, and TCM predicted asymmetries across all other global measures.

The $L + R$ Measure significantly predicted the regional AI in 87% (128/148) of volumes, in 89% (66/74) of surface areas, and in 91% (91/74) of mean thicknesses. The L-R TCM significantly predicted the regional AI in 91% (135/148) of volumes, 81% (60/74) of surface areas, and 99% (73/74) of mean thicknesses. Finally, the TCM significantly predicted the regional AI in 85% (126/148) of volumes, 93% (69/74) of surface areas, and 89% (66/74) of mean thicknesses.

Since the $L + R$ Measure, the L-R TCM, and the TCM were significant predictors ($p < 0.05$) of asymmetry in more than 5% of the investigated global and regional AIs, we concluded that the above predictors should be included when examining group differences in asymmetry and did so in the subsequent analyses.

3.2. Q2: is the relationship of the AI with the L + R measure, or with global brain size, or with the L-R TCM, non-linear?

The reduction in RSE was only greater than 1% in 2% of regions (6/306). The reduction in RSE was the greatest between the linear model and the smooth thin-plate spline (Supplemental Tables C1–4, Summary in C5). Since the reduction in RSE was more than 1% in less than 5% of the investigated global and regional AIs, we concluded that linear models were sufficient to model the relationship between AI and the $L + R$ Measure, global brain size (e.g., TBV), and the L-R TCM, which were negligibly non-linear. We conducted exploratory analyses to identify the cerebral predictors responsible for the reduction in RSE in the six regions that had a reduction in RSE that was larger than 1% (Supplemental Section 4).

3.3. Q3: to what extent do group estimates change with the included covariates?

We examined whether group differences change as a function of the predictors included in the model by comparing the magnitude and significance of the standardized sex betas obtained from Eqs. (8) to 11 (Supplemental Tables D1–4). Removing either the $L + R$ Measure or the TCM significantly changed the magnitude of the sex differences in asymmetry ($p < 0.05$) in 42% of regions (130/306 and 129/305, respectively; Fig. 1). Removing the L-R TCM also significantly changed the magnitude of the sex differences in asymmetry ($p < 0.05$) but only in 13% of regions (39/305; Fig. 1).

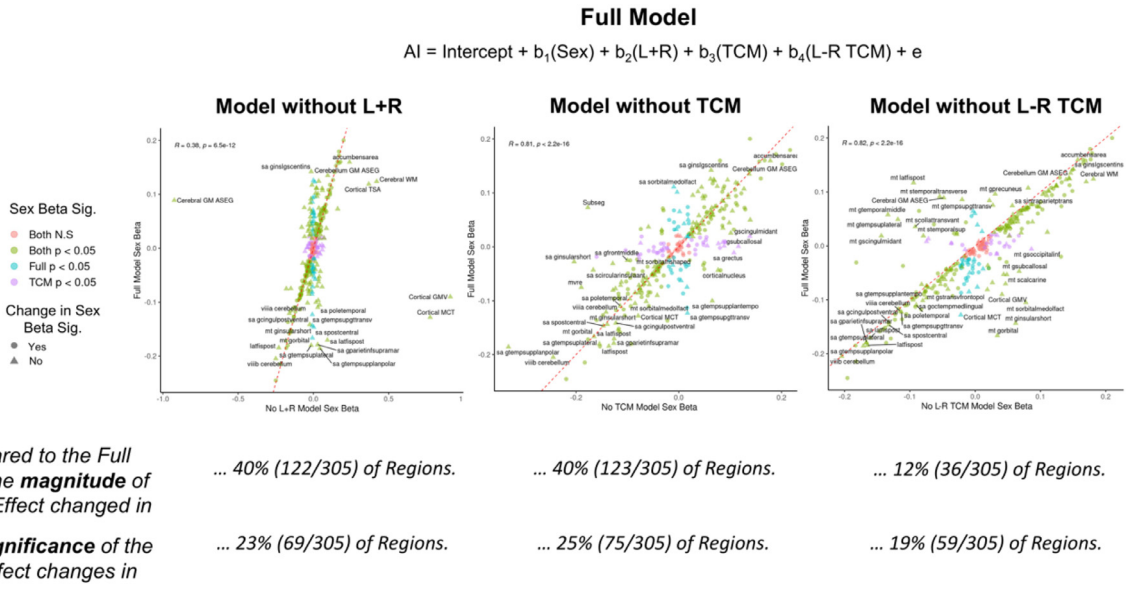

Fig. 1. *Change in the Significance and Magnitude of the Group Difference, here sex, in Asymmetry across Global and Regional Measures when removing either TCM, L + R, or L-R, TCM from the regression model.* TCM: Total Cerebral Measure, L: Left, R: Right. 305 regions without Total Brain Volume.

When looking at these results for volumes, mean thicknesses, and surface areas, separately, the estimate of the sex differences in asymmetry significantly changed in 49% (72/148) of volumes when omitting TBV, in 7% (11/148) of volumes when omitting the TBV AI, and in 9% (13/148) of volumes when omitting the $L + R$ Measure. The estimate of sex differences in asymmetry significantly changed in 69% (51/74) of surface areas when omitting TSA and in 78% (58/74) of surface areas when omitting the $L + R$ Measure. And the estimate of sex differences in asymmetry significantly changed in 34% (25/74) of mean thicknesses when omitting the Total MCT AI and in 69% (51/74) of surface areas when omitting the $L + R$ Measure. The magnitude of the sex difference in asymmetry did not change when removing the TSA AI from the model on surface areas or when removing Total MCT from the model on mean thicknesses.

The correlation of the sex estimates from the full and partial models differed across measures and indices (Supplemental File S10). For instance, correlations across models were high for regional volumes (r = 0.85 - 0.98), whereas the correlations between the sex estimates of the full model and the model without $L + R$ were not significant for surface areas (r = 0.09) and mean thicknesses (r = 0.13). The correlation between the sex estimates of the full model and the estimate of the model without L-R TCM was not significant for mean thicknesses (r = −0.09). These results are consistent with the findings, for instance, that the magnitude of the sex beta changes in a large number of mean thicknesses when estimating the sex effect without the L-R TCM (Supplemental Table D4).

We additionally examined whether removing a cerebral predictor changed the significance of the sex differences in asymmetry on all 305 regions (i.e., all regions except for TBV since the $L + R$ measure and TCM of TBV are equivalent). Removing a cerebral predictor changed the significance of the sex differences in about 22% (p <0.05) of the investigated global and regional measures (Fig. 1, Supplemental Tables D5). We additionally report the R2, AIC, and BIC of Eqs. (8)-11 and find that the full model is more appropriate across a majority of regions (Supplemental Tables E1–4).

Therefore, we conclude from the change in significance and magnitude of the sex effect on the AIs between models in several regions that removing any of the three covariates ($L + R$ Measure, TCM, or L-R TCM) from a model investigating sex differences in regional asymmetries substantially changes the reported findings.

3.4. Q4: do cerebral asymmetries vary as a function of age and sex effects and interactions?

We preregistered that we would include cerebral predictors in the models examining age and sex effects and interactions based on the results from Q1 and Q2. Therefore, although removing TSA AI for surface areas and Total MCT for mean thicknesses did not change the magnitude of group differences in Q3, these covariates were still included in the Q4 models.

We report age and sex effects and interactions in the main text that survived the strictest preregistered Bonferroni correction ($p < 0.05 / (5 \times 306)$, where 5 reflects the number of coefficients of interest). To account for all the significance tests conducted (i.e., coefficients of interests and covariates across all regions), we examined how a correction of $0.05 < (10 \times 306)$ changed the percentage of regions with significant effects for each effect and found that the change in percentage did not exceed 1.5% (Supplemental Tables F1 and F6–8).

The effects of all predictors across all regions are available in Supplemental Tables SD1–4. Plots for significant interactions are available in Supplemental File S5. We additionally report the effect of handedness.

Across global and regional measures, there were sex differences in AI in 42% (129/306) of regions, linear age effects in AI in 35% (107/306) of regions, quadratic age effects in AI in 8% (25/306) of regions, linear age by sex interactions in 3% (10/306) of regions, and no quadratic age by sex interactions.

3.4.1. Global measures

The rightward asymmetry of total MCT and Cortical GMV decreased with age (β = 0.02 and β = 0.03, respectively), whereas the rightward asymmetry of TSA, Total Subcortical Volumes, Cerebral WMV and GMV, Cerebellum GMV (FAST), and TBV linearly increased with age (from β = −0.06 to β = −0.01). The leftward asymmetry of the cerebellar WMV decreased with age (β = −0.03). A quadratic age effect was only present for the L-R FAST Cerebellar GMV (β = 0.04).

The leftward asymmetry of the Cerebral GMV (β = 0.08) and the rightward asymmetry of Cortical GMV and Total MCT were greater in females compared to males (β = −0.08, β = −0.11, respectively). The leftward asymmetry of the Cerebellar GMV (ASEG), Cerebral WMV, TBV, and TSA, was greater in males than females (ranging from β =0.09 to β = 0.16; Supplemental Table F1). There were no sex differences in the

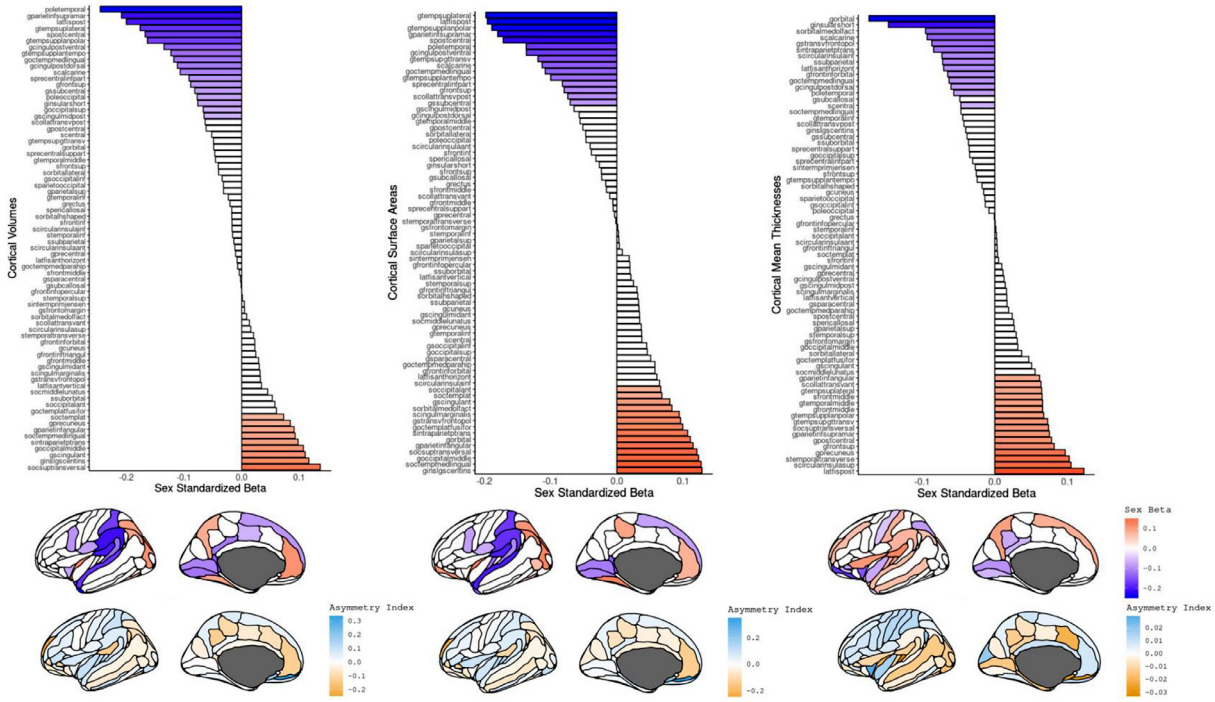

Fig. 2. *Sex Differences in Asymmetry Index (AI) across Cortical Volumes, Surface Areas, and Mean Thicknesses.* AI= (Left - Right) / (Left +Right), Males coded −0.5, Females coded 0.5. A positive sex coefficient (red) and positive AI (Left > Right; blue) indicate a greater female left-ward asymmetry. A negative sex coefficient (blue) and negative AI (Right > Left; orange) indicate a greater right-ward asymmetry in females. A positive sex coefficient (red) and a negative AI (Right > Left; orange) indicate a greater right-ward asymmetry in males. A negative sex coefficient (blue) and a positive AI (Left > Right; blue) indicate a greater male left-ward asymmetry. Colors indicate significance at $p<0.05/(5 \times 306)$. Figures made with ggseg (Mowinckel and Vidal-Piñeiro, 2019).

AI of Cerebellar WMV and GMV (FAST FSL), and Total Subcortical Volumes.

3.4.2. Cortical regions

The AI was larger in females compared to males in 12% (9/74) of cortical volumes, 19% (14/74) of surface areas, and 22% (16/74) of mean thicknesses. The AI was larger in males compared to females in 24% (18/74) of cortical volumes, 20% (15/74) of surface areas, and 19% (14/74) of mean thicknesses. The sex difference in AI ranged from −0.25 (temporal pole) to 0.14 (superior occipital sulcus and transverse occipital sulcus) for volumes, from −0.20 (posterior ramus of the lateral sulcus) to 0.13 (long insular gyrus and central sulcus of the insula) for surface areas, and from −0.17 (orbital gyrus) to 0.12 (posterior ramus of the lateral sulcus) for mean thicknesses (Fig. 2). The largest sex difference was observed in the temporal pole volume: Males had a larger leftward asymmetry than females ($\beta = -0.25$).

The AIs of males and females were very highly correlated (r>=0.98; Supplemental Information Figure S1–2) and regions with significant sex differences had asymmetries in the same direction across sexes (Supplemental Tables SG1–4) with some exceptions (Supplemental Section 5).

The AI increased with linear age in 12% (9/74) of cortical volumes, 5% (4/74) of surface areas, and 18% (13/74) of mean thicknesses. The AI decreased with linear age in 10% (7/74) of cortical volumes, 8% (5/74) of surface areas, and 15% (11/74) of mean thicknesses (Fig. 3). The rightward asymmetry of the tranverse temporal sulcus mean thickness decreased the most as linear age increased ($\beta = 0.06$), whereas the rightward asymmetry of the anterior transverse collateral sulcus surface area increased the most with linear age ($\beta = -0.06$; Fig. 3, Supplemental Figure S1).

We found a general trend for a positive age effect across the temporal parietal mean thicknesses and a negative age effect across the medial occipital-parietal mean thicknesses. Specifically, there was a decrease in the rightward AI with age in the superior temporal and parietal regions, and a decrease in leftward AI with age in some medial regions such as, the precuneus gyrus, cuneus gyrus, and paracentral gyrus and sulcus.

The AI decreased with quadratic age in the volume of the cuneus gyrus ($\beta = -0.02$), in the surface area of the short insular gyri ($\beta = 0.02$), and in the mean thicknesses of the suborbital sulcus ($\beta = 0.03$) and the inferior temporal gyrus ($\beta = 0.02$). There were no significant interactions of age by sex or age^2 by sex across cortical volumes, mean thicknesses, and surface areas.

3.4.3. Subcortical regions

Males had a larger right-ward asymmetry in the pallidum ($\beta = -0.11$) and a larger leftward asymmetry in the caudate, thalamus, and accumbens area compared to females. Females had a larger rightward asymmetry in the amygdala ($\beta = -0.16$; Fig. 4). All hippocampal subfields had an AI that was greater in females compared to males, whereas 48% (12/25) of thalamic subfields were larger in females and 16% (3/25) in males. All amygdala subfields had a larger AI in males compared to females. The subcortical AIs of regions with sex differences generally went in the same direction for both sexes (Supplemental Section 5).

The leftward asymmetry of the ventral diencephalon and the rightward asymmetry of the thalamus increased with age ($\beta = -0.06$), whereas the leftward asymmetry of the pallidum ($\beta = -0.06$), and the rightward asymmetry of the accumbens area, caudate, and hippocampus decreased with age (ranging from $\beta = -0.06$ to $\beta = -0.06$; Supplemental Table A6; Fig. 3). The thalamus AI also increased with quadratic age.

There was a significant interaction of sex with linear age in the pallidum ($\beta = 0.02$), the cortical nucleus of the amygdala ($\beta = -0.05$), the CA3 hippocampal head ($\beta = -0.06$), and the thalamic lateral geniculate ($\beta = -0.06$), ventral posterolateral ($\beta = -0.06$), mediodorsal medial magnocellular ($\beta = -0.05$), and ventral medial ($\beta = -0.06$) nuclei.

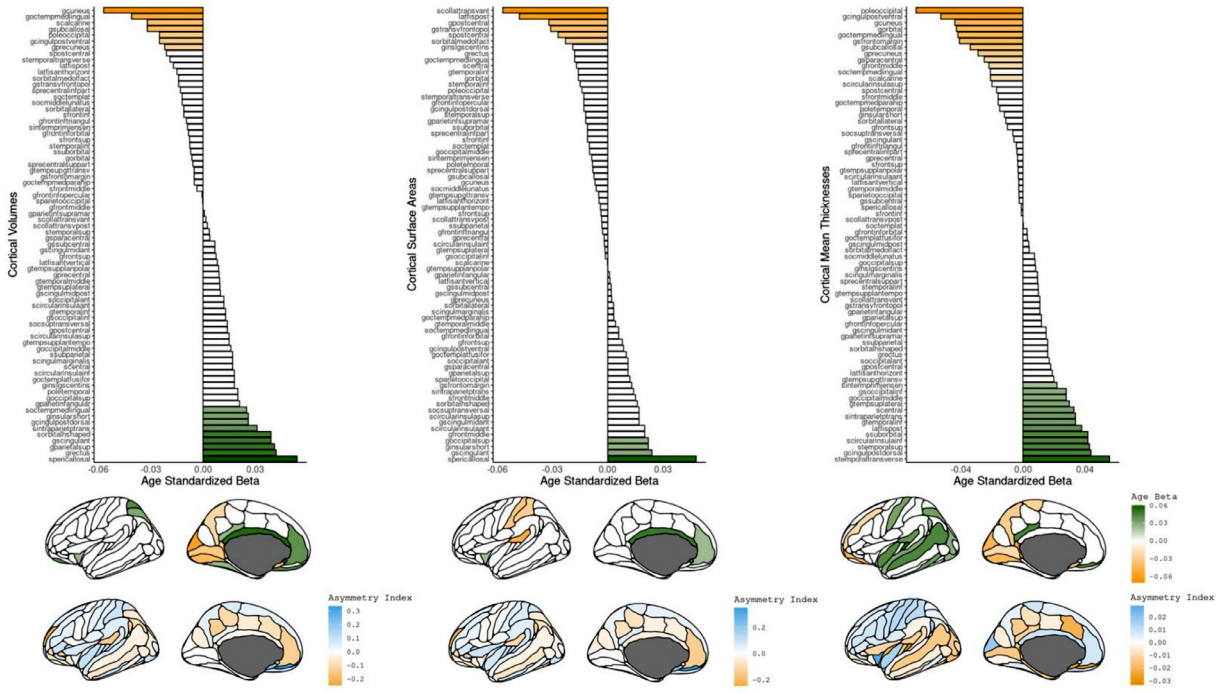

Fig. 3. *Linear Age Differences in Asymmetry Index (AI) across Cortical Volumes, Surface Areas, and Mean Thicknesses.* AI= (Left - Right) / (Left +Right). A positive age coefficient (green) and a positive AI (Left>Right; blue) indicate an increase in leftward asymmetry with increasing age. A negative age coefficient (orange) and a negative AI (Right > Left; orange) indicate an increase in rightward asymmetry with increasing age. A positive age coefficient (green) and a negative AI (Right > Left; orange) indicate a decrease in asymmetry with increasing age. A negative age coefficient (orange) and a positive AI (Left > Right; blue) indicate a decrease in asymmetry with increasing age. Colors indicate significance at $p < 0.05/(5 \times 306)$. Figures made with ggseg (Mowinckel and Vidal-Piñeiro, 2019).

3.4.4. Cerebellar gray matter volumes

Males had a larger leftward asymmetry than females in the crus I ($\beta = 0.15$) and females had a greater right-ward asymmetry in the inferior posterior Lobe (VIIIA $\beta = -0.12$, VIIIB $\beta = -0.17$). Males had a greater rightward asymmetry in the x cerebellar lobule ($\beta = -0.06$).

In the inferior posterior lobe, there was a decrease in the rightward asymmetry of lobule VIIIb ($\beta = 0.03$) and an increase in the rightward asymmetry of lobule VIIIa ($\beta = -0.04$) with age. In the superior posterior lobe, there was an increase in the crus II lobule ($\beta = 0.04$) leftward asymmetry and an increase in rightward symmetry in VIIb ($\beta = -0.04$) with age. The X lobule leftward asymmetry increased with age ($\beta = 0.04$).

The L-R VIIB and crus II lobules had a negative quadratic age effect ($\beta = -0.03$, for both) and there was a significant interaction of linear age with sex in the AIs of the crus II and X lobules ($\beta = -0.05$, $\beta = -0.06$, respectively). Males had a leftward asymmetry and females a rightward asymmetry in the VIIIB lobule ($\beta = -0.17$).

3.4.5. Handedness

We conducted exploratory analyses on handedness that are reported in supplemental section 6. In brief, AIs in 13 regions differed between left and right-handed individuals and no AI differed between right-handed and ambidextrous individuals.

4. Discussion

The present study reports the brain measures to take into consideration when examining group differences in cerebral asymmetries that are independent of brain size. We found that the $L + R$ Measure, the TCM, and the L-R TCM predict the AI of over 89% of investigated regions. The relationship between these predictors and the AIs deviated little from linearity to warrant the use of non-linear models. We used the case of sex differences in brain asymmetries to illustrate the consequences of omitting these predictors when examining group differences in asymmetries. We found that removing either the $L + R$ Measure, the TCM, or the L-R TCM changed the magnitude and significance of the sex differences in asymmetry. Finally, we reported the effects of sex, age, and their interactions when including the $L + R$ Measure, the TCM, and the L-R TCM, which, based on our results, should be considered by future studies examining group differences in brain asymmetries.

4.1. L + R *Measure*

In contrast to popular belief (X.-Z. Kong et al., 2018; F. Kurth et al., 2018), we found that dividing the L-R Measure by the $L + R$ Measure does not ensure that the index does not simply scale with brain size. Dividing the L-R Measure would sufficiently adjust for the $L + R$ Measure only if the intercept of their relationship was null. However, the intercept is not null and the $L + R$ Measure was a significant predictor of the AI. Omitting the $L + R$ Measure significantly changed the magnitude and the significance of the sex differences in 42% of regions. Thus, researchers should include the $L + R$ Measure as a covariate in their analyses of group differences in asymmetry.

If the $L + R$ Measure is included as a covariate in their model, there is no need to divide the L-R Measure by its $L + R$ Measure. One could examine brain asymmetries by analyzing L-R Measures with the appropriate covariates. However, the standard AI is convenient since it has the same scale across regions of different sizes. For this reason, we recommend using the standard AI as long as all appropriate covariates are included.

4.2. Global Brain size

Our findings corroborate the current practice of adjusting for brain size (e.g., TBV) to report group differences in cerebral asymmetry that are independent of individual differences in global brain size. In line with previous studies (Guadalupe et al., 2017; Kang et al., 2015; X.-Z. Kong et al., 2018), TCM was a significant predictor of a majority of regions, even when including the $L + R$ Measure in the model. Although

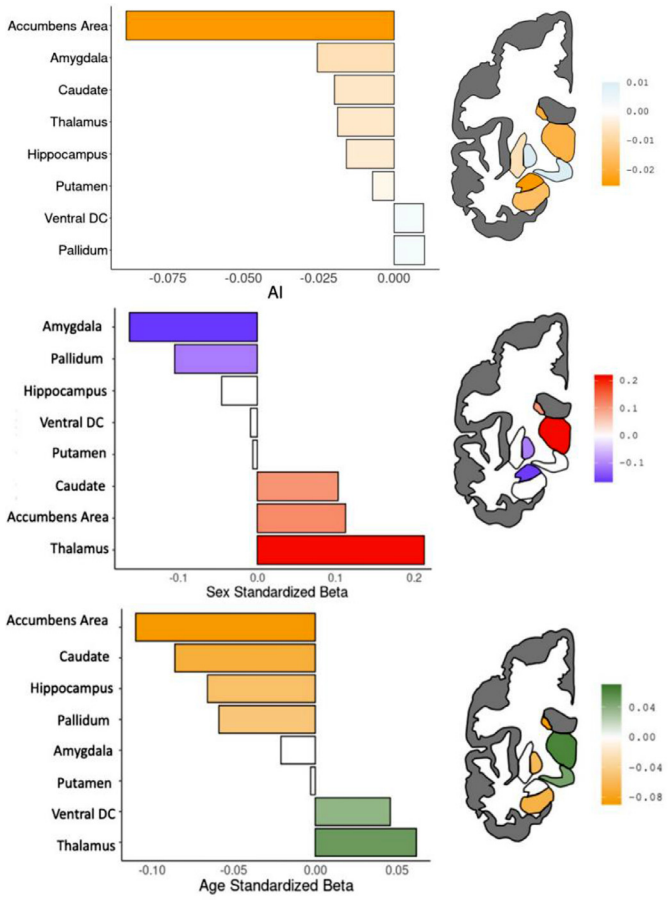

Fig. 4. *Sex and Linear Age Differences in Asymmetry Index (AI) across Subcortical Volumes.* AI= (Left - Right) / (Left +Right). A positive age coefficient (green) and AI (Left>Right; blue) indicate an increase in asymmetry with increasing age. A negative age coefficient (yellow) and AI (Right > Left; orange) indicate an increase in asymmetry with increasing age. A positive age coefficient (green) and a negative AI (Right > Left; orange) indicate a decrease in asymmetry with increasing age. A negative age coefficient (yellow) and a positive AI (Left > Right; blue) indicate a decrease in asymmetry with increasing age. Males coded −0.5; Females coded 0.5. A positive sex coefficient (red) and positive AI (Left > Right; blue)) indicate a greater female left-ward asymmetry. A negative sex coefficient (blue) and negative AI (Right > Left; orange) indicate a greater right-ward asymmetry in females. A positive sex coefficient (red) and a negative AI (Right > Left; orange) indicate a greater right-ward asymmetry in males. A negative sex coefficient (blue) and a positive AI (Left>Right; blue) indicate a greater male left-ward asymmetry. Colors indicate significance at 0.05/(5 × 306). Figures made with ggseg (Mowinckel and Vidal-Piñeiro, 2019).

Kong and colleagues (X.-Z. 2018) found an effect of ICV on the AI of overall cortical thickness but not on the AI of overall surface area, we found that TBV predicted both overall surface area and mean thickness, with greater asymmetries in larger brains.

While omitting TCM influenced the magnitude of the sex effect in volumes and surface areas, it did not influence the magnitude of the sex differences in AIs across cortical mean thicknesses. This may be because mean thickness is quite small, allowing for little variability across individuals. Removing total MCT nonetheless influenced the significance of the sex effects: four regions that were significant in the model with all the covariates were no longer significant when removing total MCT and one significant region in the model without total MCT was no longer significant in the model with all the covariates. Therefore, we suggest that Total MCT be maintained as a covariate when investigating sex differences in asymmetries. Finally, since Total MCT is a significant predictor of asymmetry across 97% of mean thicknesses, omitting Total MCT could influence the magnitude and significance of other grouping variables of interest and should be taken into account by future studies.

4.3. L-R TCM

To our knowledge, this paper is the first to examine the effects of global brain asymmetry (L-R TCM) on group differences in regional asymmetries. We found that the asymmetry between the left and the right TCMs predicts the AI of a majority of regions (85%). However, removing the L-R TCM only changed the magnitude of the reported sex differences in 13% of regions in asymmetry, generally across volumes and mean thicknesses but not surface areas. When removing the L-R TCM from the model with the cerebral covariates and sex, the sex effect became significant in 41 regions and was no longer significant in 34 regions compared to the full model. Therefore, we recommend that the L-R TCM still be considered when investigating sex differences in surface areas to disentangle global from local differences in asymmetry. Finally, since the L-R TSA is a significant predictor of the asymmetry in 81% of surface areas, omitting the L-R TSA could influence the magnitude and significance of other grouping variables of interest and so should be considered as a covariate by future studies.

These analyses lead us to recommend that studies of brain asymmetry systematically adjust on all three covariates: $L + R$ Measure, TCM, and L-R TCM. In essence, this amounts to studying residual asymmetries: asymmetries once global brain size and asymmetry factors are taken into account. Some investigators may feel that absolute asymmetries are more relevant for their purposes, or perhaps more functionally significant. They may be. The problem is that when group differences in absolute regional AI are found, one does not know whether those differences are specific to this region, or whether they are due to differences in region size, brain size, or global brain asymmetry. By comparing models with and without these covariates, researchers will assess the extent to which observed effects are regional, and the extent to which they are global, allowing for a more fine-grained understanding of variations in brain asymmetries. We applied this approach to a systematic study of the relation between residual cerebral asymmetries and sex, age and handedness in the UK Biobank, with the following results.

4.4. Sex effects

Asymmetries in males and females were generally in the same direction and the majority of sex differences reflected a more pronounced asymmetry pattern in one sex compared to the other. Consistent with Kong and colleagues (F. 2018) and Koelkebeck and colleagues (2014), we found that males have a greater rightward asymmetry in overall surface area compared to females, beyond that expected from the differences in brain size. In line with Kong and colleagues (X.-Z. 2018), we found a more pronounced leftward asymmetry in the superior-temporal surface areas across the Desikan-Killiany-Trouville (DKT) and the Destrieux atlases. We additionally reported a greater rightward asymmetry in females compared to males in the inferior parietal gyrus of the DKT atlas and the angular gyrus of the Destrieux atlas. We did not find a sex difference in asymmetry in the mean thickness of the enthorinal and parahippocampal mean thicknesses as indicated by Kong and colleagues (X.-Z. 2018), nor did we find a sex difference in the putamen as suggested by Guadalupe and colleagues (2017). These different results between our study and the literature can be explained by differences in raw AIs (e.g., putamen) or differences between samples (e.g., sample age).

With such a large dataset, we reported more significant sex differences in asymmetries than in previous studies (Guadalupe et al., 2015; Koelkebeck et al., 2014; Kong et al., 2020): We found 55 regions with greater asymmetries in women and 67 with greater asymmetries in

males. Although sex differences in asymmetries were generally consistent across segmentation algorithms and models, there were some exceptions: We observed a greater leftward asymmetry in males in the superior frontal gyrus surface area in the Destrieux atlas but not with the DKT atlas. We also only reported sex differences in the asymmetry of mean thicknesses in the superior temporal gyrus, rostral middle frontal gyrus, and the paracentral gyrus when the L-R TCM and $L + R$ Measure were included in the models. These results further highlight the importance of adjusting for these brain measures to report sex differences in regional asymmetries that are independent of brain size and global asymmetry.

There was a general pattern whereby sex effects across surface areas were reversed for mean thicknesses. The superior frontal cortex on the medial side and the temporal-parietal junction had a greater leftward asymmetry in males across surface areas and have a greater rightward asymmetry in females across mean thicknesses. The oppositive pattern was found in the lateral orbitofrontal cortex.

The presence of sex differences in cortical thickness asymmetry across regions of the language network, such as the supramarginal gyrus, the temporal transverse sulcus, planum polare of the superior temporal gyrus, and the anterior transverse temporal gyrus of Heschl, contrasts with Kong and colleagues' (X.-Z. 2018) finding. They did not report sex differences in these regions and, in turn, hypothesized that sex differences in the asymmetry of cortical thicknesses were independent of sex differences in performance on language tasks. Further structural and functional studies are needed to evaluate whether sex differences in linguistic skills are associated with sex differences in asymmetries across the volumes, surface areas, and/or cortical thicknesses of regions in the language network.

4.5. Age effects

The influence of age on brain asymmetries in the UK Biobank varied across brain measures. For instance, we found relatively more age effects across cortical mean thicknesses (24/74) than surface areas (9/74), which coincides with the hypothesis that age effects on volume are mostly driven by cortical thinning (see Storsve et al., 2014). We also found a decrease in the leftward asymmetry in temporal-parietal mean thicknesses and a decrease in the rightward asymmetry of some posterior medial mean thicknesses (e.g., precuneus and cuneus gyri). This general decrease in mean thickness asymmetry with age is consistent with a longitudinal aging study that reported a decrease in the anterior-posterior pattern of left-right thickness asymmetry between 60 and 75 years old, the age of UK Biobank participants. The authors proposed that this pattern may reflect a system-wide loss of asymmetry (Roe et al., 2021).

In contrast with Kong and colleagues' (X.-Z. 2018) study, we did not find a greater leftward asymmetry with increasing age in the surface area of the entorhinal cortex. Instead, we found a greater leftward asymmetry with increasing age in the surface areas and volumes of the cingulate regions and rightward asymmetry with increasing age in the surface areas and volumes of the postcentral gyrus and sulcus and the posterior ramus of the lateral sulcus. Considering that we are (to our knowledge) the only ones with Kong and colleagues (X.-Z. 2018) to report age effects across surface area asymmetries, our findings must be replicated to be judged as robust.

Although we reported subcortical AIs in the same direction as Guadalupe and colleagues (2107), we did not find an age effect in the AI of the putamen. Instead, we found a negative age effect on the AIs of several regions, including the caudate, whose decrease in left-ward asymmetry with age has previously been documented (Y. Wang et al., 2019). In line with Wang and colleagues (Y. 2019), we also found a general decrease in the asymmetry of the hippocampus with age. However, this decrease in asymmetry only occurred in females in their sample. Finally, we found that asymmetries in the cerebellum generally increased with age, except in the lobule VIIIb.

4.6. Handedness

Our exploratory results further support that handedness – one of the most evident functional lateralization patterns (Papadatou-Pastou et al., 2020)– was not associated with the majority of investigated asymmetries in volumes, mean thicknesses, and surface areas. Although our findings coincide with the latest large-scale studies examining brain lateralization with similar asymmetry indices (Guadalupe et al., 2017; X.-Z. Kong et al., 2018), we similarly found an effect of handedness in the surface areas of the anterior medial cingulate regions and the mean thicknesses of the postcentral region (Sha et al., 2021). Cerebral asymmetries may nonetheless more systematically vary as a function of handedness when measured by other indices. For instance, a recent study using an automated registration-based approach reported that the horizontal and vertical skew (L-R differences along the anterior-posterior and dorsal-ventral axes, respectively) differed between left- and right-handed individuals in the UK Biobank and Human Connectomes Project (X.-Z. Kong et al., 2018).

4.7. Implications

Our findings have implications that go beyond brain asymmetries. First, our results suggest that well-established indices or methods can be improved. Although the AI is an easily interpretable index that is comparable across regions, we need a model to account for the complex relationship between a regional asymmetry and regional and global brain size. Second, the paper's statistical approach reflects the systematic steps we encourage researchers to take when building models to accurately address their research questions. As larger databases become available, researchers can build more complex models and must select appropriate confounders from a large array of variables based on their pertinence while avoiding redundancy. This is particularly difficult when variables, such as cerebral ones, have complex and sometimes bidirectional relationships. Therefore, when selecting confounding variables, we recommend evaluating the possible underlying relationships between variables in light of the question at hand, with the hope of reducing the likelihood of reporting spurious estimates and facilitating interpretation.

4.8. Limitations

The UK Biobank dataset consists of older adults that are healthier and have a higher socioeconomic status than the UK population (Fry et al., 2017). The UK Biobank imaging sample also shows a healthy bias compared to the UK Biobank sample (Lyall et al., 2021) and may underestimate exposure and outcome estimates (Lyall et al., 2021). Therefore, even with proper adjustment for cerebral covariates, group differences in asymmetry in the current UK Biobank sample may not be generalizable to the UK population. As a cross-sectional study in older adults, the present study is also limited in its ability to study age related changes in asymmetries. In light of these limitations, we present the largest study of sex and age effects and interactions on brain asymmetries in older adults. We appropriately controlled for individual differences in brain size and used data from a few imaging sites with similar MRI scanner characteristics and acquisition sequences, reducing the likelihood of obtaining biased estimates from different imaging parameters.

4.9. Conclusion

We find that the widely-used AI significantly scales with brain size. Using the case of sex differences, we illustrate that the $L + R$ Measure, the TCM, and the L-R TCM should be considered to report unbiased

group differences in cerebral asymmetries. Taking into account the appropriate covariates will not only shed light on debated brain asymmetries across healthy controls but also on the variations in brain asymmetry associated with differences in cognition and mental health. Although numerous studies examining the link between mental health disorders and asymmetry find that, given the small effect sizes, structural brain asymmetry alone is unlikely to be a useful biomarker of many disorders for individual-level prediction or diagnosis (Kong et al., 2020; Postema et al., 2021) studying brain asymmetry may contribute to understanding the neurobiological underpinnings of cognition and psychiatric disorders.

Camille M. Williams: Conceptualization, Methodology, Software, Formal analysis, Data Curation, Writing - Original Draft, Writing - Review & Editing, Visualization.

Franck Ramus, Hugo Peyre: Conceptualization, Methodology, Writing - Original Draft, Writing - Review & Editing, Supervision.

Roberto Toro: Methodology, Writing - Original Draft, Writing - Review & Editing.

Data/Code availability

This research has been conducted using data from UK Biobank, a major biomedical database (http://www.ukbiobank.ac.uk/). Restrictions apply to the availability of these data, which were used under license for this study: application 46,007. Preregistration, supplemental tables and information, and code are available here: https://osf.io/nqz4h/.

Ethics approval statement

All participants provided informed consent ("Resources tab" at https://biobank.ctsu.ox.ac.uk/crystal/field.cgi?id=200). The UK Biobank received ethical approval from the Research Ethics Committee (reference 11/NW/0382) and the present study was conducted based on application 46 007.

Supporting information

Figure SA-SI.

Declaration of Competing Interest

On behalf of all authors, the corresponding author states that there is no conflict of interest.

Acknowledgments

This work received support under the program "Investissements d'Avenir" launched by the French Government and implemented by l'Agence Nationale de la recherche (ANR) with the references ANR-17-EURE-0017 and ANR-10-IDEX-0001–02 PSL. Funding was also obtained from Fondation pour l'Audition (FPA RD-2016–8 research grant). This research has been conducted using the UK Biobank Resource. Declarations of interest: none.

Supplementary materials

Supplementary material associated with this article can be found, in the online version, at doi:10.1016/j.neuroimage.2022.119118.

References

Alfaro-Almagro, F., Jenkinson, M., Bangerter, N.K., Andersson, J.L.R., Griffanti, L., Douaud, G., Sotiropoulos, S.N., Jbabdi, S., Hernandez-Fernandez, M., Vallee, E., Vidaurre, D., Webster, M., McCarthy, P., Rorden, C., Daducci, A., Alexander, D.C., Zhang, H., Dragonu, I., Matthews, P.M., … Smith, S.M., 2018. Image processing and Quality Control for the first 10,000 brain imaging datasets from UK Biobank. Neuroimage 166, 400–424. doi:10.1016/j.neuroimage.2017.10.034.

Altarelli, I., Leroy, F., Monzalvo, K., Fluss, J., Billard, C., Dehaene-Lambertz, G., Galaburda, A.M., Ramus, F., 2014. Planum temporale asymmetry in developmental dyslexia: Revisiting an old question. Hum. Brain Mapp. 35 (12), 5717–5735. doi:10.1002/hbm.22579.

Cherbuin, N., Réglade-Meslin, C., Kumar, R., Sachdev, P., Anstey, K.J., 2010. Mild Cognitive Disorders are Associated with Different Patterns of Brain asymmetry than Normal Aging: The PATH through Life Study. Frontiers in Psychiatry 1, 00. doi:10.3389/fpsyt.2010.00011.

de Kovel, C.G.F., Lisgo, S., Karlebach, G., Ju, J., Cheng, G., Fisher, S.E., Francks, C., 2017. Left–Right Asymmetry of Maturation Rates in Human Embryonic Neural Development. Biol. Psychiatry 82 (3), 204–212. doi:10.1016/j.biopsych.2017.01.016.

Finlay, B.L., Darlington, R.B., Nicastro, N., 2001. Developmental structure in brain evolution. Behav. Brain Sci. 24 (2), 263–278. doi:10.1017/S0140525X01003958, discussion 278-308.

Fish, A.M., Cachia, A., Fischer, C., Mankiw, C., Reardon, P.K., Clasen, L.S., Blumenthal, J.D., Greenstein, D., Giedd, J.N., Mangin, J.-.F., Raznahan, A., 2017. Influences of Brain Size, Sex, and Sex Chromosome Complement on the Architecture of Human Cortical Folding. Cereb. Cortex 27 (12), 5557–5567. doi:10.1093/cercor/bhw323.

Fjell, A.M., Westlye, L.T., Amlien, I., Espeseth, T., Reinvang, I., Raz, N., Agartz, I., Salat, D.H., Greve, D.N., Fischl, B., Dale, A.M., Walhovd, K.B., 2009. Minute Effects of Sex on the Aging Brain: A Multisample Magnetic Resonance Imaging Study of Healthy Aging and Alzheimer's Disease. J. Neurosci. 29 (27), 8774–8783. doi:10.1523/JNEUROSCI.0115-09.2009.

Fry, A., Littlejohns, T.J., Sudlow, C., Doherty, N., Adamska, L., Sprosen, T., Collins, R., Allen, N.E., 2017. Comparison of Sociodemographic and Health-Related Characteristics of UK Biobank Participants With Those of the General Population. Am. J. Epidemiol. 186 (9), 1026–1034. doi:10.1093/aje/kwx246.

Galaburda, A.M., Corsiglia, J., Rosen, G.D., Sherman, G.F., 1987. Planum temporale asymmetry, reappraisal since Geschwind and Levitsky. Neuropsychologia 25 (6), 853–868. doi:10.1016/0028-3932(87)90091-1.

Guadalupe, T., Mathias, S.R., vanErp, T.G.M., Whelan, C.D., Zwiers, M.P., Abe, Y., Abramovic, L., Agartz, I., Andreassen, O.A., Arias-Vásquez, A., Aribisala, B.S., Armstrong, N.J., Arolt, V., Artiges, E., Ayesa-Arriola, R., Baboyan, V.G., Banaschewski, T., Barker, G., Bastin, M.E., … Francks, C., 2017. Human subcortical brain asymmetries in 15,847 people worldwide reveal effects of age and sex. Brain Imaging and Behavior 11 (5), 1497–1514. doi:10.1007/s11682-016-9629-z.

Guadalupe, T., Zwiers, M.P., Wittfeld, K., Teumer, A., Vasquez, A.A., Hoogman, M., Hagoort, P., Fernandez, G., Buitelaar, J., van Bokhoven, H., Hegenscheid, K., Völzke, H., Franke, B., Fisher, S.E., Grabe, H.J., Francks, C., 2015. Asymmetry within and around the human planum temporale is sexually dimorphic and influenced by genes involved in steroid hormone receptor activity. Cortex 62, 41–55. doi:10.1016/j.cortex.2014.07.015.

Kang, X., Herron, T.J., Ettlinger, M., Woods, D.L., 2015. Hemispheric asymmetries in cortical and subcortical anatomy. Laterality 20 (6), 658–684. doi:10.1080/1357650X.2015.1032975.

Kavaklioglu, T., Guadalupe, T., Zwiers, M., Marquand, A.F., Onnink, M., Shumskaya, E., Brunner, H., Fernandez, G., Fisher, S.E., Francks, C., 2017. Structural asymmetries of the human cerebellum in relation to cerebral cortical asymmetries and handedness. Brain Structure and Function 222 (4), 1611–1623. doi:10.1007/s00429-016-1295-9.

Koelkebeck, K., Miyata, J., Kubota, M., Kohl, W., Son, S., Fukuyama, H., Sawamoto, N., Takahashi, H., Murai, T., 2014. The contribution of cortical thickness and surface area to gray matter asymmetries in the healthy human brain. Hum. Brain Mapp. 35 (12), 6011–6022. doi:10.1002/hbm.22601.

Kong, X.-.Z., Mathias, S.R., Guadalupe, T., Glahn, D.C., Franke, B., Crivello, F., Tzourio-Mazoyer, N., Fisher, S.E., Thompson, P.M., Francks, CENIGMA Laterality Working Group, 2018. Mapping cortical brain asymmetry in 17,141 healthy individuals worldwide via the ENIGMA Consortium. Proc. Nat. Acad. Sci. U.S.A. 115 (22), E5154–E5163. doi:10.1073/pnas.1718418115.

Kong, X.-.Z., Postema, M.C., Guadalupe, T., de Kovel, C., Boedhoe, P.S.W., Hoogman, M., Mathias, S.R., van Rooij, D., Schijven, D., Glahn, D.C., Medland, S.E., Jahanshad, N., Thomopoulos, S.I., Turner, J.A., Buitelaar, J., van Erp, T.G.M., Franke, B., Fisher, S.E., van den Heuvel, O.A., … Francks, C. (2020). Mapping brain asymmetry in health and disease through the ENIGMA consortium. Human Brain Mapping. doi:10.1002/hbm.25033.

Kurth, F., Thompson, P.M., Luders, E., 2018. Investigating the differential contributions of sex and brain size to gray matter asymmetry. Cortex 99, 235–242. doi:10.1016/j.cortex.2017.11.017.

Lefebvre, A., Beggiato, A., Bourgeron, T., Toro, R., 2015. Neuroanatomical Diversity of Corpus Callosum and Brain Volume in Autism: Meta-analysis, Analysis of the Autism Brain Imaging Data Exchange Project, and Simulation. Biol. Psychiatry 78 (2), 126–134. doi:10.1016/j.biopsych.2015.02.010.

Leonard, C.M., Voeller, K.K.S., Lombardino, L.J., Morris, M.K., Hynd, G.W., Alexander, A.W., Andersen, H.G., Garofalakis, M., Honeyman, J.C., Mao, J., Agee, O.F., Staab, E.V., 1993. Anomalous Cerebral Structure in Dyslexia Revealed With Magnetic Resonance Imaging. Arch. Neurol. 50 (5), 461–469. doi:10.1001/archneur.1993.00540050013008.

Liu, D., Johnson, H.J., Long, J.D., Magnotta, V.A., & Paulsen, J.S. (2014). The power-proportion method for intracranial volume correction in volumetric imaging analysis. Frontiers in Neuroscience, 8. doi:10.3389/fnins.2014.00356.

Luders, E., Narr, K.L., Thompson, P.M., Rex, D.E., Jancke, L., Toga, A.W., 2006. Hemispheric Asymmetries in Cortical Thickness. Cereb. Cortex 16 (8), 1232–1238. doi:10.1093/cercor/bhj064.

Lyall, D., Quinn, T., Lyall, L.M., Ward, J., Anderson, J., Smith, D., Stewart, W., Strawbridge, R.J., Bailey, M., Cullen, B., 2021. Quantifying bias in psychological and physical health in the UK Biobank imaging sub-sample. PsyArXiv doi:10.31234/osf.io/upvb9.

Maingault, S., Tzourio-Mazoyer, N., Mazoyer, B., Crivello, F., 2016. Regional correlations between cortical thickness and surface area asymmetries: A surface-based morphometry study of 250 adults. Neuropsychologia 93, 350–364. doi:10.1016/j.neuropsychologia.2016.03.025.

Mazoyer, B., Zago, L., Jobard, G., Crivello, F., Joliot, M., Perchey, G., Mellet, E., Petit, L., Tzourio-Mazoyer, N., 2014. Gaussian Mixture Modeling of Hemispheric Lateralization for Language in a Large Sample of Healthy Individuals Balanced for Handedness. PLoS One 9 (6), e101165. doi:10.1371/journal.pone.0101165.

Miller, K.L., Alfaro-Almagro, F., Bangerter, N.K., Thomas, D.L., Yacoub, E., Xu, J., Bartsch, A.J., Jbabdi, S., Sotiropoulos, S.N., Andersson, J.L.R., Griffanti, L., Douaud, G., Okell, T.W., Weale, P., Dragonu, I., Garratt, S., Hudson, S., Collins, R., Jenkinson, M., … Smith, S.M., 2016. Multimodal population brain imaging in the UK Biobank prospective epidemiological study. Nat. Neurosci. 19 (11), 1523–1536. doi:10.1038/nn.4393.

Mowinckel, A.M., & Vidal-Piñeiro, D. (2019). Visualisation of Brain Statistics with R-packages ggseg and ggseg3d. ArXiv:1912.08200 [Stat]. http://arxiv.org/abs/1912.08200

Ocklenburg, S., Schmitz, J., Moinfar, Z., Moser, D., Klose, R., Lor, S., Kunz, G., Tegenthoff, M., Faustmann, P., Francks, C., Epplen, J.T., Kumsta, R., Güntürkün, O., 2017. Epigenetic regulation of lateralized fetal spinal gene expression underlies hemispheric asymmetries. ELife 6, e22784. doi:10.7554/eLife.22784.

Papadatou-Pastou, M., Ntolka, E., Schmitz, J., Martin, M., Munafò, M.R., Ocklenburg, S., Paracchini, S., 2020. Human handedness: A meta-analysis. Psychol. Bull. 146 (6), 481–524. doi:10.1037/bul0000229.

Perperoglou, A., Sauerbrei, W., Abrahamowicz, M., Schmid, M., 2019. A review of spline function procedures in R. BMC Med. Res. Method. 19 (1), 46. doi:10.1186/s12874-019-0666-3.

Plessen, K.J., Hugdahl, K., Bansal, R., Hao, X., Peterson, B.S., 2014. Sex, Age, and Cognitive Correlates of Asymmetries in Thickness of the Cortical Mantle Across the Life Span. The Journal of Neuroscience 34 (18), 6294–6302. doi:10.1523/JNEUROSCI.3692-13.2014.

Postema, M.C., Hoogman, M., Ambrosino, S., Asherson, P., Banaschewski, T., Bandeira, C.E., Baranov, A., Bau, C.H.D., Baumeister, S., Baur-Streubel, R., Bellgrove, M.A., Biederman, J., Bralten, J., Brandeis, D., Brem, S., Buitelaar, J.K., Busatto, G.F., Castellanos, F.X., Cercignani, M., … Francks, C., 2021. Analysis of structural brain asymmetries in attention-deficit/hyperactivity disorder in 39 datasets. Journal of Child Psychology and Psychiatry, and Allied Disciplines 62 (10), 1202–1219. doi:10.1111/jcpp.13396.

Reardon, P.K., Clasen, L., Giedd, J.N., Blumenthal, J., Lerch, J.P., Chakravarty, M.M., Raznahan, A., 2016. An Allometric Analysis of Sex and Sex Chromosome Dosage Effects on Subcortical Anatomy in Humans. J. Neurosci. 36 (8), 2438–2448. doi:10.1523/JNEUROSCI.3195-15.2016.

Reardon, P.K., Seidlitz, J., Vandekar, S., Liu, S., Patel, R., Park, M.T.M., Alexander-Bloch, A., Clasen, L.S., Blumenthal, J.D., Lalonde, F.M., Giedd, J.N., Gur, R.C., Gur, R.E., Lerch, J.P., Chakravarty, M.M., Satterthwaite, T.D., Shinohara, R.T., Raznahan, A., 2018. Normative brain size variation and brain shape diversity in humans. Science 360 (6394), 1222–1227. doi:10.1126/science.aar2578.

Roe, J.M., Vidal-Piñeiro, D., Sørensen, Ø., Brandmaier, A.M., Düzel, S., Gonzalez, H.A., Kievit, R.A., Knights, E., Kühn, S., Lindenberger, U., Mowinckel, A.M., Nyberg, L., Park, D.C., Pudas, S., Rundle, M.M., Walhovd, K.B., Fjell, A.M., Westerhausen, R., 2021. Asymmetric thinning of the cerebral cortex across the adult lifespan is accelerated in Alzheimer's disease. Nat. Commun. 12, 721. doi:10.1038/s41467-021-21057-y.

Sanchez-Roige, S., Palmer, A.A., Fontanillas, P., Elson, S.L., Adams, M.J., Howard, D.M., Edenberg, H.J., Davies, G., Crist, R.C., Deary, I.J., McIntosh, A.M., Clarke, T.-.K., 2019. Genome-Wide Association Study Meta-Analysis of the Alcohol Use Disorders Identification Test (AUDIT) in Two Population-Based Cohorts. Am. J. Psychiatry 176 (2), 107–118. doi:10.1176/appi.ajp.2018.18040369.

Sanchis-Segura, C., Ibañez-Gual, M.V., Adrián-Ventura, J., Aguirre, N., Gómez-Cruz, Á.J., Avila, C., Forn, C., 2019. Sex differences in gray matter volume: How many and how large are they really? Biology of Sex Differences 10 (1), 32. doi:10.1186/s13293-019-0245-7.

Sha, Z., Schijven, D., Carrion-Castillo, A., Joliot, M., Mazoyer, B., Fisher, S.E., Crivello, F., & Francks, C. (2021). The genetic architecture of structural left–right asymmetry of the human brain. Nature Human Behaviour, 1–14. doi:10.1038/s41562-021-01069-w.

Steinmetz, H., Rademacher, J., Huang, Y.X., Hefter, H., Zilles, K., Thron, A., Freund, H.J., 1989. Cerebral asymmetry: MR planimetry of the human planum temporale. J. Comput. Assist. Tomogr. 13 (6), 996–1005.

Storsve, A.B., Fjell, A.M., Tamnes, C.K., Westlye, L.T., Overbye, K., Aasland, H.W., Walhovd, K.B., 2014. Differential Longitudinal Changes in Cortical Thickness, Surface Area and Volume across the Adult Life Span: Regions of Accelerating and Decelerating Change. The Journal of Neuroscience 34 (25), 8488–8498. doi:10.1523/JNEUROSCI.0391-14.2014.

Sudlow, C., Gallacher, J., Allen, N., Beral, V., Burton, P., Danesh, J., Downey, P., Elliott, P., Green, J., Landray, M., Liu, B., Matthews, P., Ong, G., Pell, J., Silman, A., Young, A., Sprosen, T., Peakman, T., Collins, R., 2015. UK Biobank: An Open Access Resource for Identifying the Causes of a Wide Range of Complex Diseases of Middle and Old Age. PLoS Med. 12 (3), e1001779. doi:10.1371/journal.pmed.1001779.

Toga, A.W., Thompson, P.M., 2003. Mapping brain asymmetry. Nat. Rev. Neurosci. 4 (1), 37–48. doi:10.1038/nrn1009.

Toro, R., Chupin, M., Garnero, L., Leonard, G., Perron, M., Pike, B., Pitiot, A., Richer, L., Veillette, S., Pausova, Z., Paus, T., 2009. Brain volumes and Val66Met polymorphism of the BDNF gene: Local or global effects? Brain Structure & Function 213 (6), 501–509. doi:10.1007/s00429-009-0203-y.

Wang, Y., Xu, Q., Luo, J., Hu, M., Zuo, C., 2019. Effects of Age and Sex on Subcortical Volumes. Frontiers in Aging Neuroscience 11, 00. https://www.frontiersin.org/article/10.3389/fnagi.2019.00259.

Williams, C.M., Peyre, H., Toro, R., Ramus, F., 2021a. Neuroanatomical norms in the UK Biobank: The impact of allometric scaling, sex, and age. Hum. Brain Mapp. 42 (14), 4623–4642. doi:10.1002/hbm.25572.

Williams, C.M., Peyre, H., Toro, R., & Ramus, F. (2021b). Sex differences in the brain are not reduced to differences in body size. Neuroscience & Biobehavioral Reviews. doi:10.1016/j.neubiorev.2021.09.015.

Wood, S.N. (2017). Generalized Additive Models: An Introduction with R (2nd ed.). Chapman and Hall/CRC. doi:10.1201/9781315370279.

Zago, L., Petit, L., Jobard, G., Hay, J., Mazoyer, B., Tzourio-Mazoyer, N., Karnath, H.-.O., Mellet, E., 2017. Pseudoneglect in line bisection judgement is associated with a modulation of right hemispheric spatial attention dominance in right-handers. Neuropsychologia 94, 75–83. doi:10.1016/j.neuropsychologia.2016.11.024.

Zuo, Z., Ran, S., Wang, Y., Li, C., Han, Q., Tang, Q., Qu, W., Li, H., 2019. Asymmetry in cortical thickness and subcortical volume in treatment-naïve major depressive disorder. NeuroImage: Clinical 21, 101614. doi:10.1016/j.nicl.2018.101614.